NOTES AND CORRESPONDENCE

A Satellite Perspective of the 3 May 1999 Great Plains Tornado Outbreak within Oklahoma

DAN BIKOS, JOHN WEAVER,* AND BRIAN MOTTA

Cooperative Institute for Research in the Atmosphere, Colorado State University, Fort Collins, Colorado

28 February 2001 and 18 September 2001

ABSTRACT

Geostationary Operational Environmental Satellite (GOES) imagery from 3 May 1999 is examined. Synoptic-scale water vapor imagery shows a deepening low-amplitude upper-level trough over the western United States on 3 May, which develops a negative tilt as a jet streak digs south-southeastward over California. The imagery also shows a second jet streak propagating rapidly from Baja California to the southern Great Plains. This feature intensifies as it propagates into the diffluent region on the east side of the trough. Thunderstorms initiate as this jet streak moves over western Oklahoma during the late afternoon. GOES visible imagery shows a north–south cloud boundary over southwestern Oklahoma on 3 May. To the west of this boundary, cumulus cloudiness dominates. To the east, stratocumulus and wave (billow) clouds characterize the low-level cloud field. As the jet streak and associated cirrus propagate over northern Texas, towering cumulus clouds develop and then dissipate. As the cirrus clouds propagate over western Oklahoma, towering cumulus clouds develop and persist. This note discusses important features observed in GOES imagery as it pertains to convective morphology. These features were not adequately resolved by the numerical models but were important in the forecast. The benefits of using satellite imagery in combination with model output and other data are discussed.

1. Introduction

On 3 May 1999, a major tornado outbreak occurred over the central plains of the United States. Many large and damaging tornadoes occurred in Oklahoma, Kansas, and northern Texas, with 77 tornadoes being observed across the region (NCDC 1999). A total of 46 people died and 825 were injured. Many homes and businesses were damaged or destroyed, with the total dollar damage estimate now reaching $1.2 billion. For Oklahoma, the tornado count makes this outbreak the largest ever recorded in the state.

This note examines the utility of Geostationary Operational Environmental Satellite (GOES) imagery in identifying aspects of the synoptic and mesoscale environments not well resolved by numerical models. Water vapor imagery will be shown to reveal an upper-level jet streak that moved into Oklahoma at the time of convective initiation. Jet streaks can be important to severe convective outbreaks. Fawbush et al. (1951) observed that one of the conditions favorable for tornado development is the intersection of the vertical projection of an upper-level jet with the axis of a low-level moisture ridge. Early researchers such as Beebe and Bates (1955), Lee and Galway (1958), and others addressed the correlation between the exit region of upper jets and severe storms. Upper-tropospheric jets have been shown to provide a mechanism for convective destabilization (Newton 1967; Uccellini and Johnson 1979; Kocin et al. 1986). Forecast operational model output on 3 May greatly understated the intensity and misplaced the position of this jet streak.

GOES visible imagery will be utilized to delineate differing air masses that provide focusing mechanisms for intensifying later convection. The imagery presented will show a dryline forming near the Oklahoma–Texas border during the afternoon and will reveal new convection forming beneath the leading edge of the cirrus cloudiness of the jet streak as it moves into the region during the early afternoon. This new convection devel-

* Additional affiliation: NOAA/NESDIS/RAMM Team, Fort Collins, Colorado.

Corresponding author address: Dan Bikos, Regional and Mesoscale Meteorology team, Cooperative Institute for Research in the Atmosphere, Colorado State University, W. Laporte Avenue, Fort Collins, CO 80523-1375.
E-mail: bikos@cira.colostate.edu

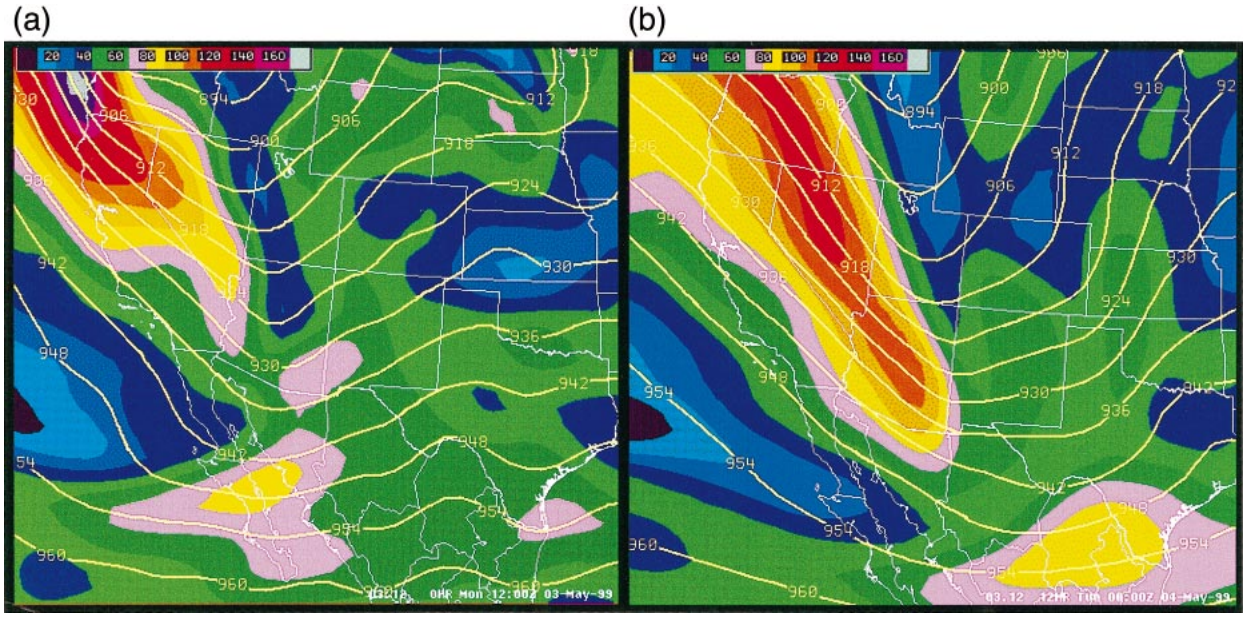

FIG. 1. Eta Model 300-hPa heights and isotachs for (a) 0-h forecast valid at 1200 UTC 3 May 1999 and (b) 12-h forecast valid 0000 UTC 4 May 1999.

oped into supercells that produced the destructive tornadoes in central Oklahoma.

2. Synoptic overview

Upper-air analyses from 1200 UTC on 3 May 1999 depicted an intensifying long-wave trough over the western United States. A large jet maximum was digging south along the northern California coast, and a smaller jet maximum was analyzed along the southern Arizona and New Mexico border (Fig. 1a). GOES water vapor imagery shows a patch of cirrus associated with the smaller jet streak farther to the south over northern Mexico (Fig. 2a), and GOES-derived wind fields[1] (Fig. 2b) confirm that the jet streak actually was farther south than shown in the Eta Model initial analysis. Also, notice that the Eta 0-h forecast wind speeds show a maximum of 70 kt in southern Arizona, whereas the GOES-derived winds show speeds as high as 85 kt. At 500 hPa, the Eta 0-h forecast (Fig. 3) shows a short-wave trough over northern Arizona associated with the large jet streak.

The Eta 12-h forecast for 0000 UTC 4 May 1999 suggests that the center of the smaller jet streak would move into southwest Kansas (Fig. 1b) and weaken. The winds at and above 500 hPa (which were 65 kt, or less, on the Norman, Oklahoma, 1200 UTC 3 May 1999 sounding) were not expected to increase (cf. Figs. 1a and 1b). In addition, the Eta 500-hPa negative vorticity center was forecast to move into central Oklahoma (Fig. 4) ahead of the approaching short wave. The vertical velocity forecast at 500 hPa (not shown) shows subsidence associated with negative vorticity advection into the afternoon, suppressing deep convection early in the afternoon. Last, the Eta 12-h forecast surface-based CAPE shows a minimum over central Oklahoma (Fig. 5), though values were over 2000 J kg^{-1}.

This situation illustrates why forecasters should not use model forecasts of CAPE by themselves—a simultaneous examination of model-predicted convection is required to be sure that model-generated convection has not erroneously decreased CAPE values. The 1200 UTC sounding analysis from Norman (not shown) had an estimated late-afternoon CAPE value of more than 3000 J kg^{-1} and an observed 0–3-km storm-relative helicity of 122 m^2 s^{-2}. These factors indicated a likelihood of severe weather over the region; however, there was considerable uncertainty in the details of convective initiation and mode based on the early-morning data (Thompson and Edwards 2000).

The Storm Prediction Center (SPC) day-1 convective outlook issued at 1246 UTC stated that there was a slight risk of severe thunderstorms for portions of the south central plains, including Oklahoma. Their discussion mentioned ''large-scale ascent'' associated with the arrival of the northern Arizona short wave after 2300 UTC. However, the forecasters thought that the destabilization in Oklahoma was overdone by the models (though the CAPE forecast available at this time was from the 0000 UTC run). Furthermore, their discussion stated that the upper winds would back during the late

[1] Wind vectors are computed from a sequence of three water vapor images using the U.S. Navy Operational Global Atmospheric Prediction System model as the first-guess field. For a description of this product see Velden et al. (1997).

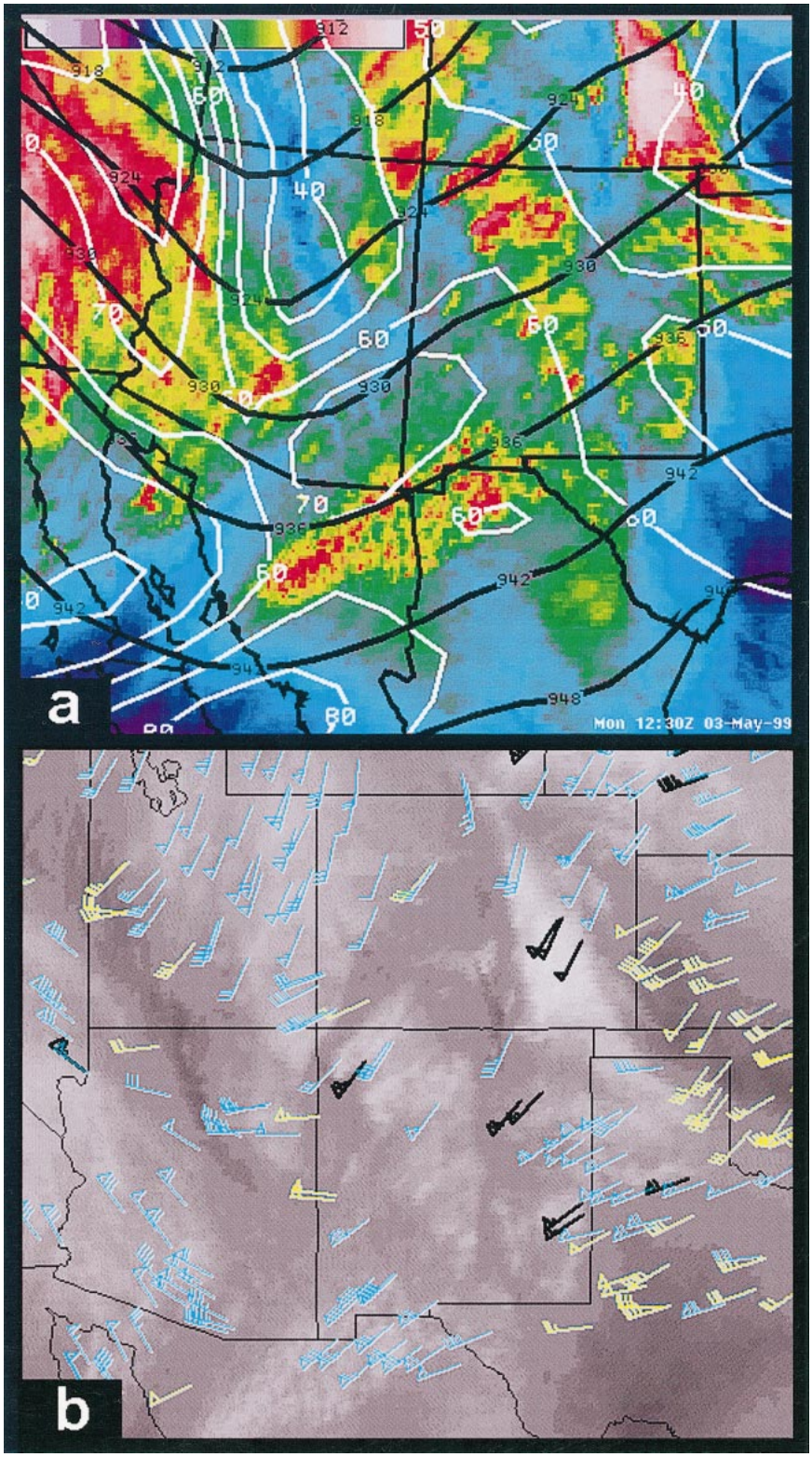

FIG. 2. *GOES-10* 6.7-μm water vapor image taken at 1230 UTC 3 May 1999 overlain with (a) Eta Model 0-h forecast of 300-hPa heights and isotachs at 1200 UTC 3 May 1999 and (b) GOES-derived winds. Black barbs are in the 100–250-hPa layer, cyan barbs are in the 251–350-hPa layer, and yellow barbs are in the 351–500-hPa layer. Wind speeds are in knots.

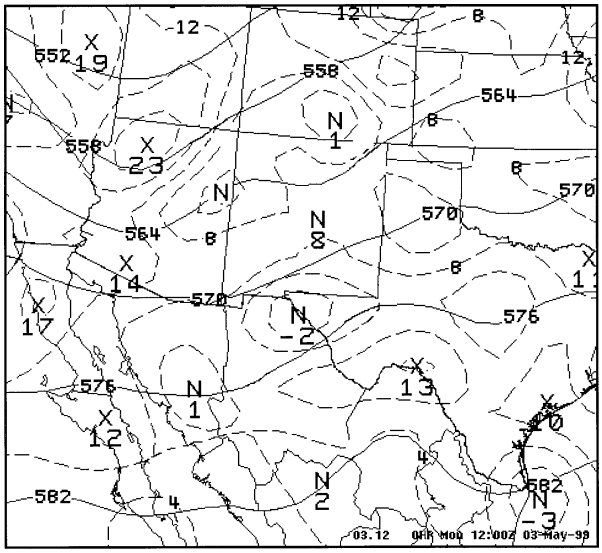

FIG. 3. Eta Model 0-h forecast of 500-hPa heights and vorticity at 1200 UTC 3 May 1999.

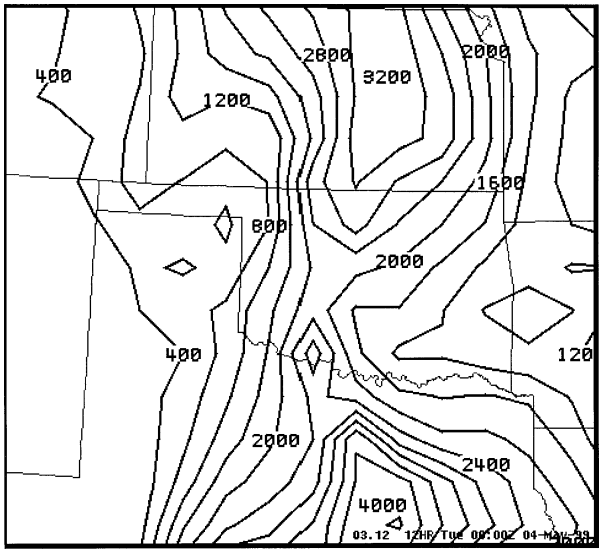

FIG. 5. Eta Model 12-h forecast of surface-based CAPE (J kg^{-1}) valid at 0000 UTC 4 May 1999.

afternoon in advance of the approaching short wave and that this backing would cause the storms to evolve toward high-precipitation supercells and then become linear. Thus, there would only be a brief window of opportunity for tornado potential. The text stated that the biggest threat would be large hail and damaging winds.

Though the SPC discussion did note that the mid- and upper-level winds on either side of the Arizona short wave were significantly underforecast by the Eta Model, it did not mention the smaller jet streak, or jet cirrus, shown in Fig. 2. In a postanalysis by Thompson and Edwards (2000), it was noted that, ''the embedded jet streak was not resolved well by operational models prior to the outbreak.''

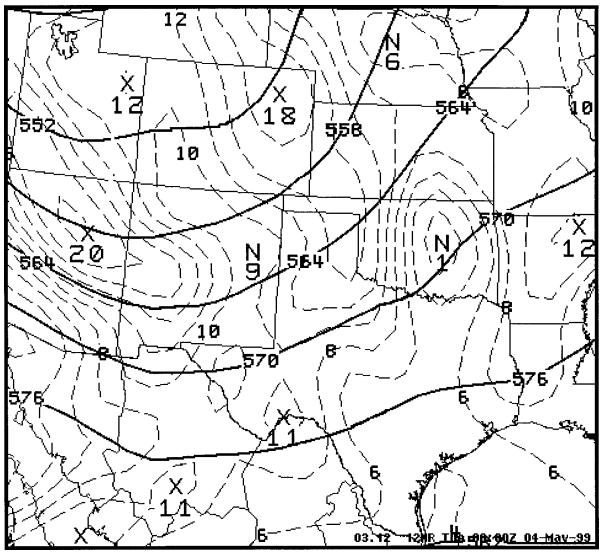

FIG. 4. Eta Model 12-h forecast of 500-hPa heights and vorticity valid at 0000 UTC 4 May 1999.

3. Afternoon convective morphology

By 1800 UTC, several factors were indicating that tornado potential was increasing. Surface-based CAPE had already exceeded Eta-predicted values. The SPC 1615 UTC discussion mentioned CAPE values of 3500–4500 J kg^{-1} over Texas and Oklahoma by late afternoon. A special sounding released from Norman at 1800 UTC (Fig. 6) showed an observed CAPE value of nearly 3000 J kg^{-1}. This destabilization is also shown by AERI–GOES[2] sounding data (Feltz et al. 1998; Feltz and Mecikalski 2002; Schmit et al. 2002) as indicated in Figs. 7 and 8. The SPC discussion also referred to an intensifying dryline in west Texas and a low-level jet east of that boundary. This situation implied not only rapid low-level moisture advection, but also the potential for increasing helicity. The discussion stated that the combination of increased instability, the low-level jet, and

[2] AERI = atmospheric emitted radiance interferometer (Smith et al. 1999). The AERI–GOES retrieval technique combines sounding retrieval information from the downlooking GOES sounder and the uplooking AERI instrument to produce a final sounding that is better than that from either instrument alone.

→

FIG. 7. AERI–GOES-derived sounding for Purcell, OK, at 1934 UTC 3 May 1999.

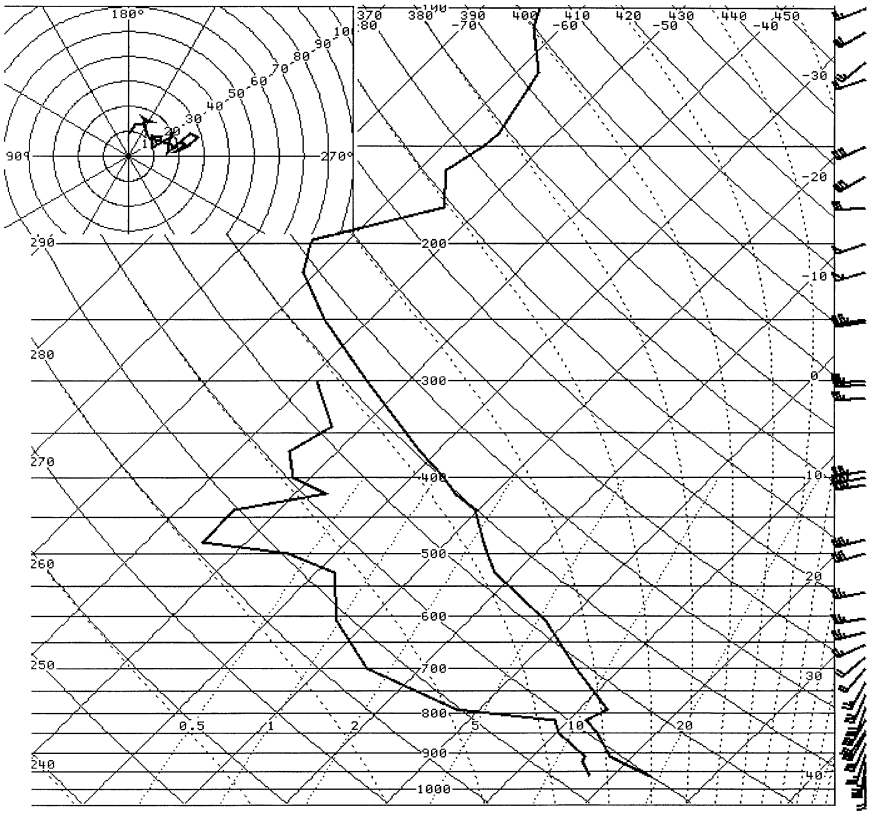

FIG. 6. Sounding from Norman, OK, at 1800 UTC 3 May 1999 plotted on a skew *T*–log*p* diagram. Wind speeds are in knots. Hodograph is plotted in the upper-left corner.

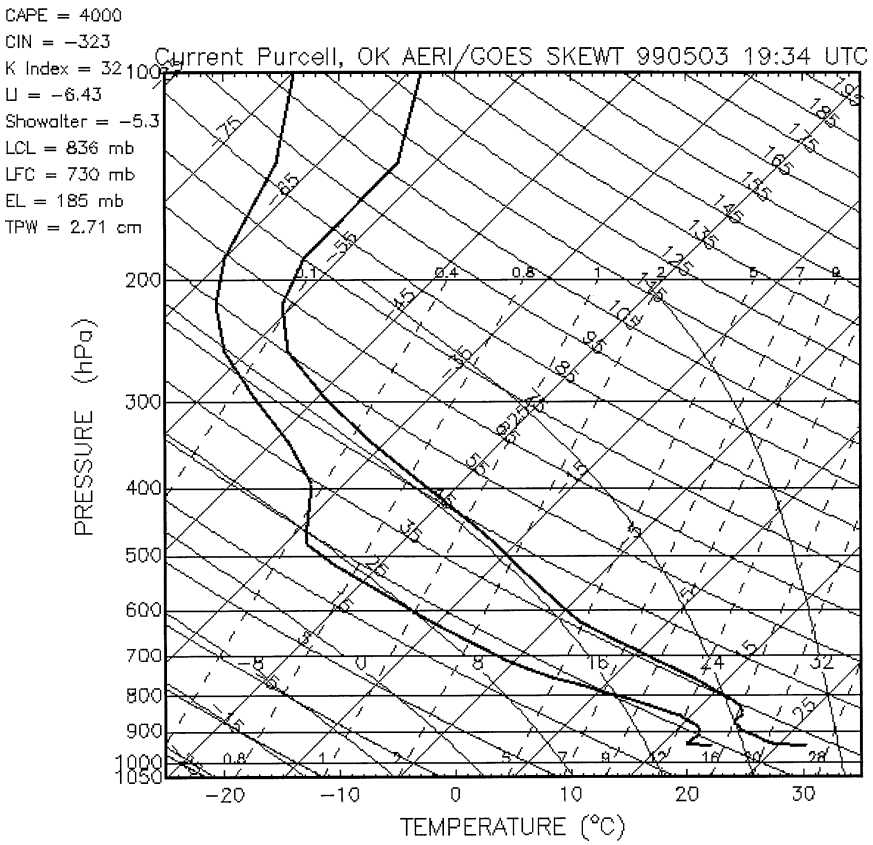

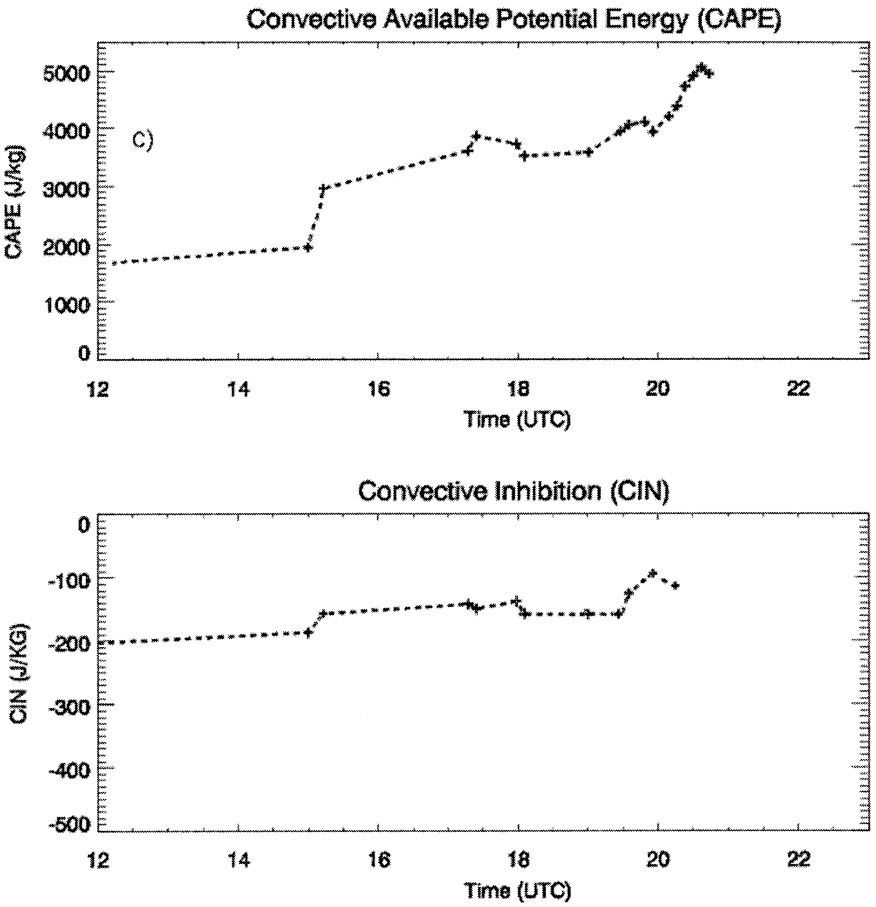

FIG. 8. AERI–GOES-derived time series of (top) CAPE and (bottom) convective inhibition at Purcell on 3 May 1999. (Figure courtesy of W. Feltz, CIMSS, Madison, WI.)

midlevel winds of 50 kt would be sufficient to support a few strong or violent tornadic supercells. Based on these new trends, the updated outlook increased the severe weather risk to ''moderate'' for the area of interest.

Satellite imagery provides even more evidence of an increasingly favorable situation. Cloud-tracking measurements from GOES water vapor imagery show that the smaller jet streak was moving northeast at 70 kt and was increasing in areal extent as indicated by a rapidly growing area of jet cirrus (Fig. 9). In this case, it is likely that the increase an area was due almost entirely to intensification, given that the dewpoints at 250 and 300 hPa were approximately the same over the entire area of interest. In the 6-h period between Figs. 2 and 9, the newly developed cirrus can be seen over eastern New Mexico and the Texas Panhandle, indicating increasing wind speeds at cloud top and associated synoptic-scale upward vertical motion. The increasing wind speed is verified by the Tucumcari, New Mexico, wind profiler (Fig. 10). GOES-derived winds give a more quantitative assessment of this intensifying jet streak (Fig. 11). The derived wind speeds in both the 100–250- and the 251–350-hPa layers were as high as 80 kt over the Texas Panhandle. Also, the analysis clearly shows lesser wind speeds to the east over Oklahoma. The area of rapidly growing cirrus associated with this approaching jet can be tracked in animated imagery as it approached Oklahoma. The operational models are less likely to represent accurately a jet streak of this size, especially considering that it originated over a data-sparse area (i.e., over the Pacific Ocean and into northern Mexico).

Visible imagery was the first data source to show newly developing convection. Figure 12 shows several important features. Thin cirrus over most of north Texas represents the leading edge of the jet streak. Notice that the cirrus is thin enough to allow us to see a small region of developing cumulus that is forming in the drier air west of the dryline (Fig. 12a). These cumulus clouds may be seen to be forming in a large clear slot in the cirrus at the leading edge of the jet. The mechanism responsible for these convective clouds is unclear in this case but may be related to inertia–gravity waves generated when the mass and momentum fields cannot adjust rapidly enough at the entrance and exit regions (Van Tuyl and Young 1982). Uccellini (1975) suggests that

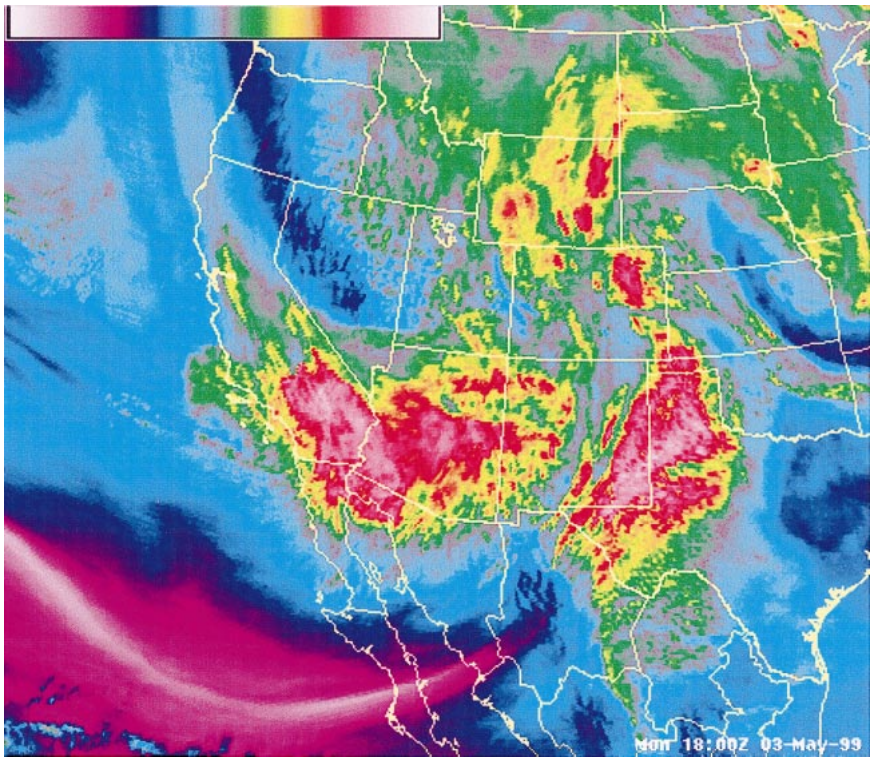

FIG. 9. *GOES-10* 6.7-μm water vapor image taken at 1800 UTC 3 May 1999.

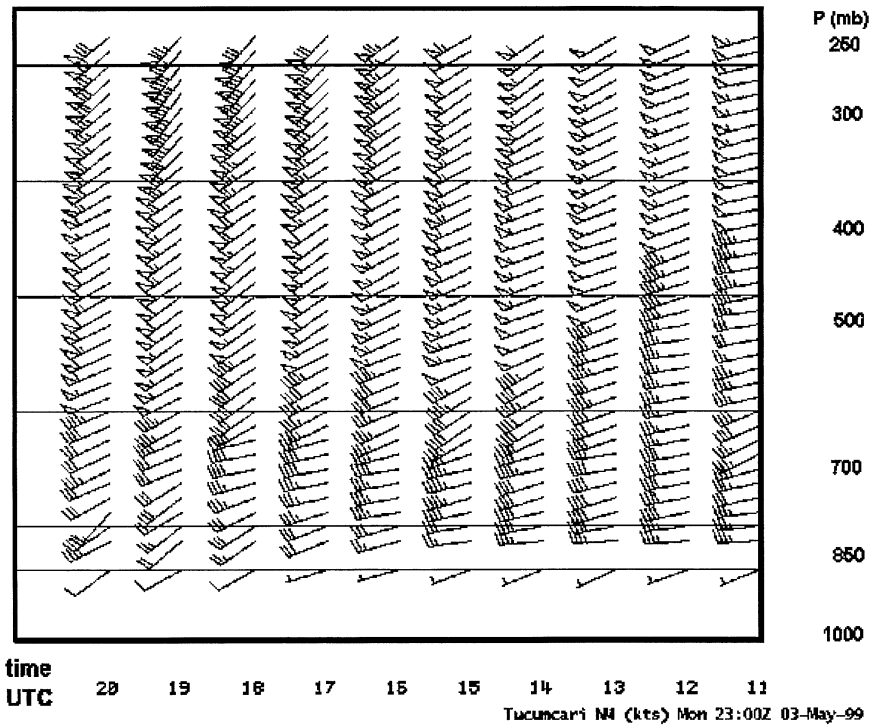

FIG. 10. Wind profiler data from Tucumcari, NM, from 1100 to 2100 UTC 3 May 1999. Wind speeds are in knots.

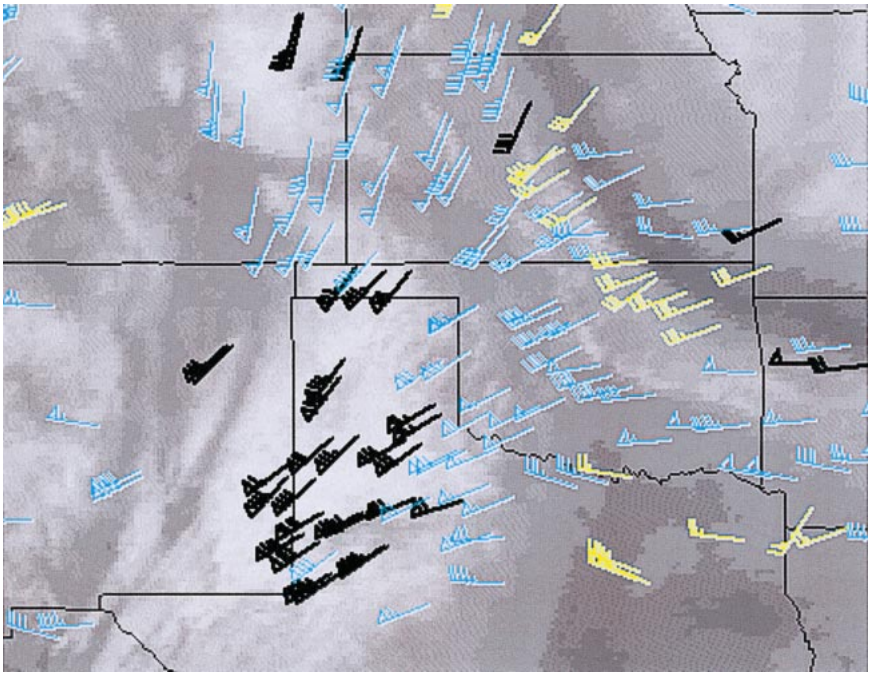

FIG. 11. GOES-derived winds at 1800 UTC 3 May 1999. Black barbs are in the 100–250-hPa layer, cyan barbs in the 251–350-hPa layer, and yellow barbs are in the 351–500-hPa layer. Wind speeds are in knots.

these jet-related gravity waves can be an important mechanism for initiation of convective storms.

Last, notice the differing air masses that may be seen over Oklahoma. Figure 12b shows these differing air masses from a *GOES-8* perspective, which allows the wave clouds to be identified more readily. The wave clouds in southeastern Oklahoma have formed in a region over which cloud cover persisted throughout the morning hours and in which Oklahoma Mesonet data (not shown) observed surface temperatures 3°–5°F cooler than the air in western Oklahoma. West of the stable wave clouds, there is a transition to cumulus cloudiness. Low-level boundaries that form at the intersection of differing air masses can be important to thunderstorm development (Scofield and Purdom 1986), thunderstorm intensity (Markowski et al. 1998), and thunderstorm movement (Weaver 1979). Our analysis of the location of this boundary agrees with that presented by Thompson and Edwards (2000) along the southern extent but disagrees to the north. Their analysis continues the boundary northward, but the satellite imagery shows it turning northeastward. The mesonet observations shown in Thompson and Edwards (2000) support the satellite analysis with backed (southerly) winds south and east of our analyzed position and southwesterly to the west and north.

The first storm in Oklahoma (herein designated storm A) formed in the southwest portion of the state. This storm would later produce the F5 damage in Moore, Oklahoma. Towering cumulus clouds in Oklahoma were first observed in visible imagery at 2015 UTC (just east-northeast of the developing storm in Texas in Fig. 13), and the first radar reflectivity echo appeared at 2042 UTC at the Frederick, Oklahoma, WSR-88D. Animated visible satellite imagery shows that this storm moved along the northeast–southwest segment of the boundary separating the stable wave clouds from the cumulus (e.g., Fig. 14). It is important to remember that the overshooting top position has been displaced northeastward relative to the ground (on *GOES-10*) by parallax. Other storms were initiated north of storm A, but none formed to the south in the area of the stable wave clouds until much later. This analysis of storm motion relative to the low-level boundary disagrees with Thompson and Edwards (2000), who suggested that the tornadic storms moved across a north–south boundary into the stable air mass before producing tornadoes. Regardless of which analysis is used, it is clear that the boundary–storm interaction was an important component.

4. Concluding remarks

The 3 May 1999 case shows the utility of satellite imagery on a number of spatial and temporal scales. Model output suggested that the magnitude of the maximum wind speed in the small jet streak approaching Oklahoma from the southwest would not increase throughout the period (Thompson and Edwards 2000). However, water vapor imagery, satellite-derived wind fields, and wind profiler data indicated an increase in

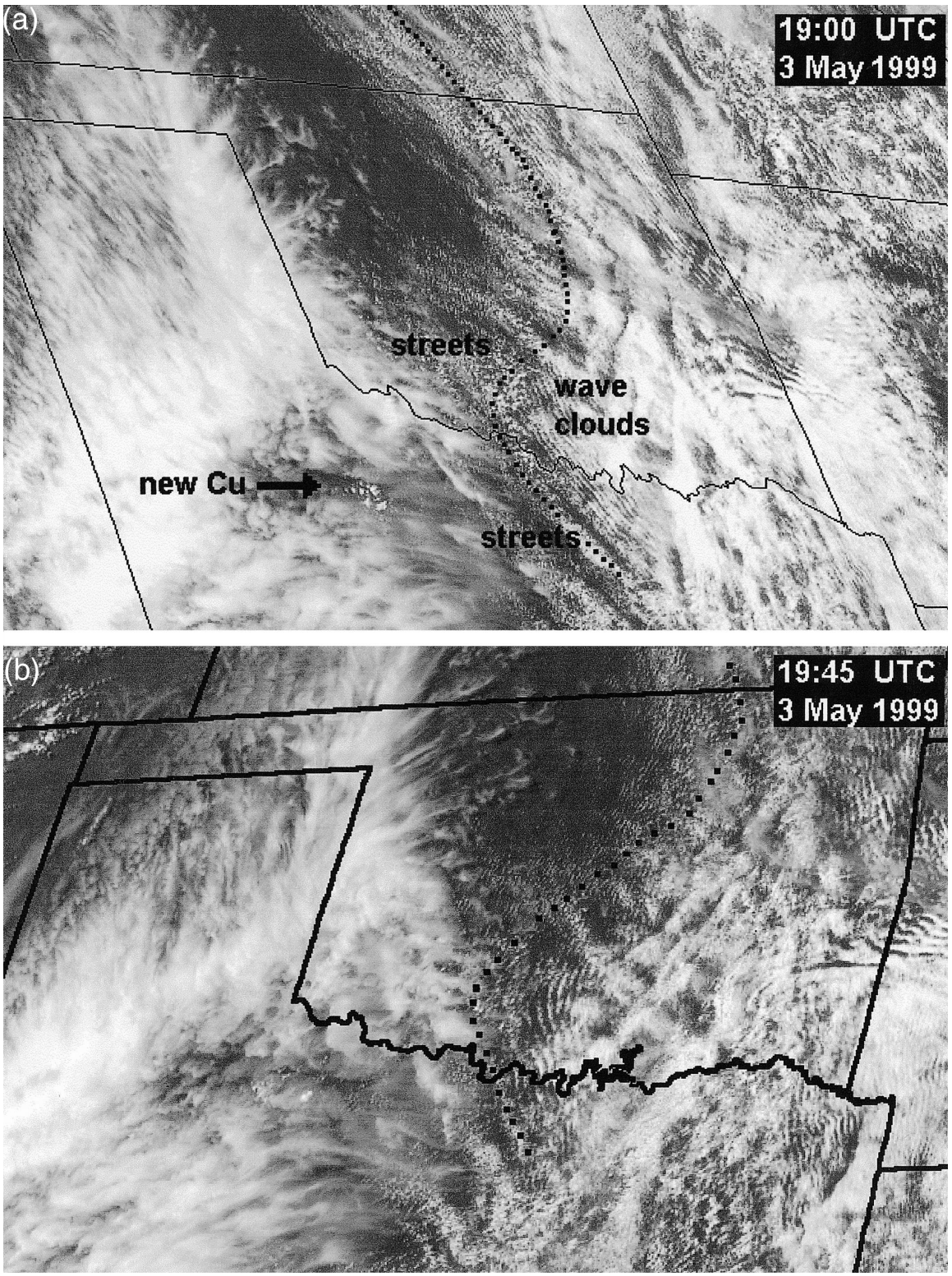

FIG. 12. (a) *GOES-10* visible satellite image at 1900 UTC 3 May 1999. Arrow points to area of developing cumulus. Areas of wave clouds and cloud streets are located as indicated. Boundary separating these two air masses is indicated by dotted line. (b) *GOES-8* visible satellite image at 1945 UTC showing many of the same features from a different vantage point.

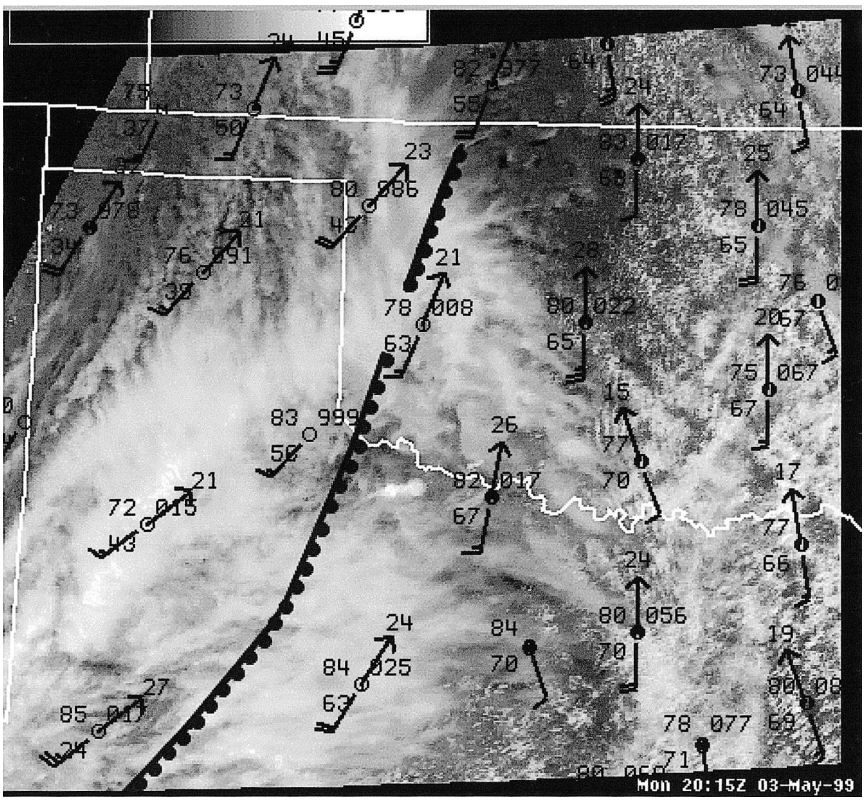

FIG. 13. *GOES-8* visible satellite image at 2015 UTC 3 May 1999. Dryline position as shown by scalloped line. Station plots are U.S. convention except that wind gusts (kt) are indicated by arrows.

the maximum wind speed. Also, satellite imagery showed an increase in the areal extent of the cirrus. The model output predicted this jet streak would move into southwest Kansas by 0000 UTC, but satellite imagery showed it to be moving through west Texas toward southwest Oklahoma. The jet streak was an important component of the outbreak. As Weisman (1999) stated in congressional testimony, the ''profiler network was especially critical on 3 May for monitoring the progression of a jet stream feature . . . which alerted forecasters to the increasing potential for very severe storms that afternoon. *Such an evolution was not anticipated using the more standard observing and modeling systems* [italics added].'' As shown in this note, satellite imagery did allow for identification and tracking of the evolution of this feature. This suggests it would be beneficial for forecasters to utilize the quantitative data provided by GOES-derived winds that can supplement traditional satellite interpretation techniques.

Model output predicted subsidence into the afternoon in the area of interest, and GOES imagery showed new convection forming as the jet streak approached. Towering cumulus clouds were observed forming even on the dry side of the dryline. Model output also suggested that CAPE values would be less than 2000 J kg^{-1} in central Oklahoma, but a special sounding released at Norman observed values of about 3000 J kg^{-1} at 1800 UTC, and AERI–GOES sounding retrievals confirmed this value. Time tendency plots of these data showed a continued increase in CAPE as the afternoon went on.

In summary, GOES imagery on 3 May revealed many critical elements of outbreak. The imagery showed (a) an intensifying jet streak approaching the area of interest that had been underforecast by the models; (b) that the jet streak, as computed by cloud-drift wind tracking, was moving northeast at 70 kt; (c) that GOES-derived winds indicated a maximum wind speed of 80 kt within the jet streak over the central Texas Panhandle and higher values farther south (d) cumulus developing and dissipating in the dry air west of the dryline as the leading edge of jet cirrus moved into the area; (e) a pre-existing mesoscale boundary separating a region of cloud streets from a region of stable wave cloudiness; and (f) new convection forming in western Oklahoma. The first tower in Oklahoma grew quickly into a large cumulonimbus, and the first tornado was reported less than 1 h later. Animated imagery indicates that storm A moved northeast, intersected the preexisting mesoscale boundary, and may have tracked along this boundary as it moved toward Oklahoma City. What role (if any) this boundary played in storm motion is not known.

Many of the important features evident on satellite

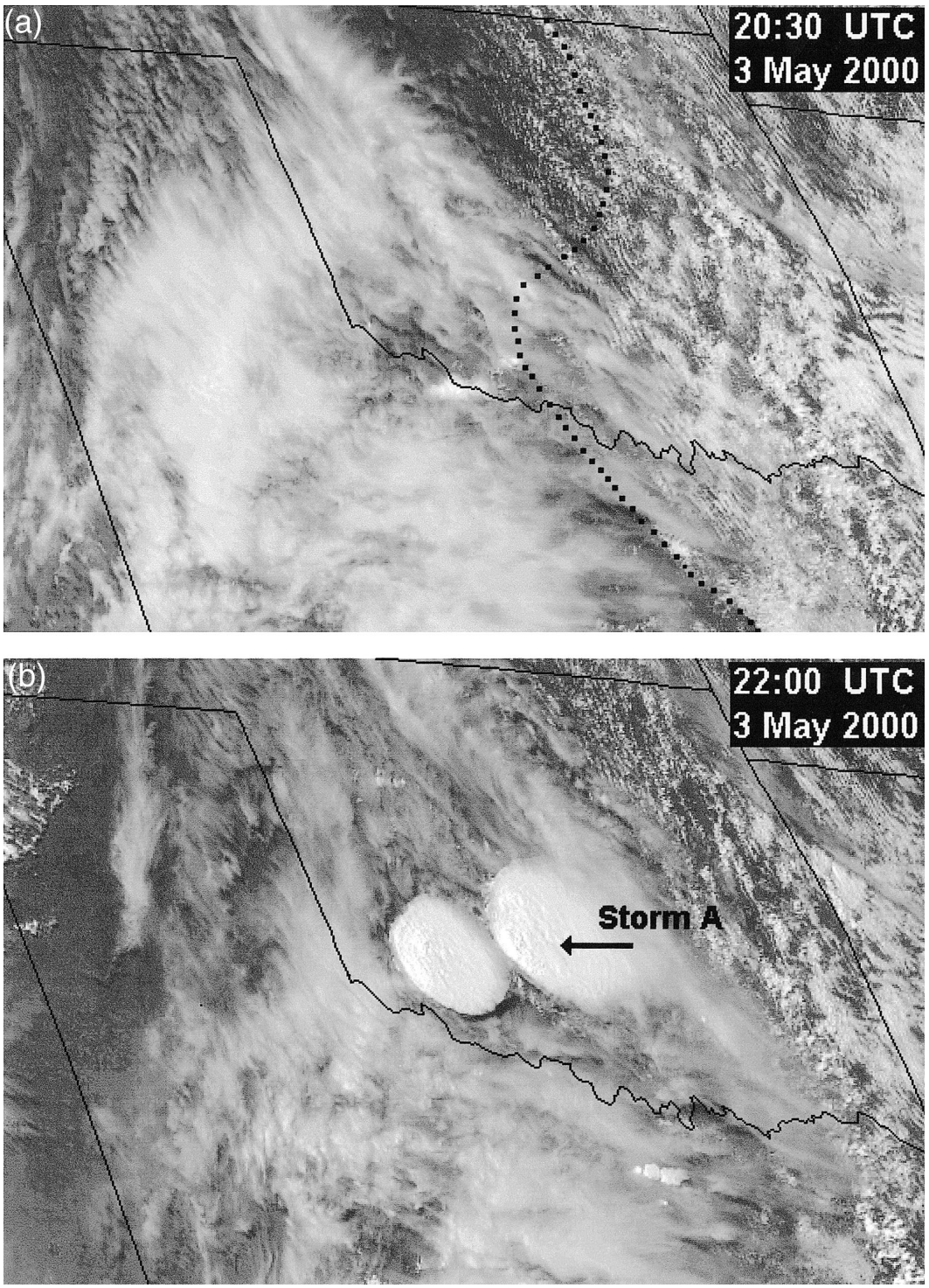

FIG. 14. *GOES-10* visible satellite imagery at (a) 2030 and (b) 2200 UTC 3 May 1999. Dotted line shows approximate position of boundary detailed in Fig. 12. Arrow points to storm A.

imagery in this case would have been useful information for the forecaster/nowcaster to have had during the rapid development and evolution of new convection. In this case, the routine GOES scanning schedule was used, and images were available every 15 min with a 9–12-min delay before they were available on Advanced Weather Interactive Processing System (AWIPS) workstations. The most beneficial mode of GOES scanning

for severe convection is rapid-scan operations (RSO). With RSO activation, double the number of images would have been available. More important, these images would have been delivered to AWIPS within 8 min. In part, because of this outbreak, the SPC now routinely requests RSO scheduling whenever the day-1 outlook calls for moderate, or greater, risk of severe weather.

Acknowledgments. A portion of the research presented in this study was performed under NOAA Grant NA67RJ0152. The authors thank Wayne Feltz of the Cooperative Institute for Meteorological Satellite Studies (CIMSS) at the University of Wisconsin—Madison for supplying data for Figs. 7 and 8 and for discussions concerning the AERI–GOES instrument and Dr. Robert Rabin (CIMSS and National Severe Storms Laboratory) for Figs. 2b and 11. The authors also express their appreciation to CIRA reviewers Dr. Mark DeMaria, Jack Dostalek, Bard Zajac, and Dr. Louis Grasso.

REFERENCES

Beebe, R. G., and F. C. Bates, 1955: A mechanism for assisting in the release of convective instability. *Mon. Wea. Rev.*, **83,** 1–10.

Fawbush, E. J., R. C. Miller, and L. G. Starrett, 1951: An empirical method of forecasting tornado development. *Bull. Amer. Meteor. Soc.*, **32,** 1–9.

Feltz, W. F., and J. R. Mecikalski, 2002: Monitoring high-temporal-resolution convective stability indices using the ground-based atmospheric emitted radiance interferometer (AERI) during the 3 May 1999 Oklahoma–Kansas tornado outbreak. *Wea. Forecasting*, **17,** 445–455.

——, W. L. Smith, R. O. Knuteson, H. R. Revercomb, H. B. Howell, and H. H. Woolf, 1998: Meteorological applications of temperature and water vapor retrievals from the ground-based atmospheric emitted radiance interferometer (AERI). *J. Appl. Meteor.*, **37,** 857–875.

Kocin, P. J., L. W. Uccellini, and R. A. Petersen, 1986: Rapid evolution of a jet streak circulation in a pre-convective environment. *Meteor. Atmos. Phys.*, **35,** 103–138.

Lee, J. T., and J. G. Galway, 1958: The jet chart. *Bull. Amer. Meteor. Soc.*, **39,** 217–223.

Markowski, P. M., E. N. Rasmussen, and J. M. Straka, 1998: The occurrence of tornadoes in supercells interacting with boundaries during VORTEX-95. *Wea. Forecasting*, **13,** 852–859.

NCDC, 1999: *Storm Data.* Vol. 41, No. 5, 371 pp. [Available from National Climatic Data Center, 151 Patton Ave., Asheville, NC 28801-5001.]

Newton, C. W., 1967: Severe convective storms. *Advances in Geophysics*, Vol. 12, Academic Press, 257–303.

Schmit, T. J., W. F. Feltz, W. P. Menzel, J. Jung, A. P. Noel, J. N. Heil, J. P. Nelson III, and G. S. Wade, 2002: Validation and use of GOES sounder moisture information. *Wea. Forecasting*, **17,** 139–154.

Scofield, R. A., and J. F. W. Purdom, 1986: The use of satellite data for mesoscale analyses and forecasting application. *Mesoscale Meteorology and Forecasting*, P. S. Ray, Ed., Amer. Meteor. Soc., 118–150.

Smith, W. L., W. F. Feltz, R. O. Knuteson, H. R. Revercomb, H. B. Howell, and H. H. Woolf, 1999: The retrieval of planetary boundary layer structure using ground-based infrared spectral radiance measurements. *J. Atmos. Oceanic Technol.*, **16,** 323–333.

Thompson, R. L., and R. Edwards, 2000: An overview of environmental conditions and forecast implications of the 3 May 1999 tornado outbreak. *Wea. Forecasting*, **15,** 682–699.

Uccellini, L. W., 1975: A case study of apparent gravity wave initiation of severe convective storms. *Mon. Wea. Rev.*, **103,** 497–513.

——, and D. Johnson, 1979: The coupling of upper and lower tropospheric jet streaks and implications for the development of severe convective storms. *Mon. Wea. Rev.*, **107,** 682–703.

Van Tuyl, A. H., and J. A. Young, 1982: Numerical simulation of nonlinear jet streak adjustment. *Mon. Wea. Rev.*, **110,** 2038–2054.

Velden, C. S., C. M. Hayden, S. J. Nieman, W. P. Menzel, S. Wanzong, and J. S. Goerss, 1997: Upper-tropospheric winds derived from geostationary satellite water vapor observations. *Bull. Amer. Meteor. Soc.*, **78,** 173–195.

Weaver, J. F., 1979: Storm motion as related to boundary-layer convergence. *Mon. Wea. Rev.*, **107,** 612–619.

Weisman, M. L., 1999: Testimony for Tornadoes: Understanding, Modeling, and Forecasting Supercell Storms before the House Subcommittee on Basic Research, Committee on Science. 106 Cong., 16 June.